

Received:
29 August 2017
Revised:
6 December 2017
Accepted:
29 January 2018

Cite as: N. Jmail,
M. Zaghoud, A. Hadriche,
T. Frikha, C. Ben Amar,
C. Bénar. Integration of
stationary wavelet transform
on a dynamic partial
reconfiguration for recognition
of pre-ictal gamma
oscillations.
Heliyon 4 (2018) e00530.
doi: [10.1016/j.heliyon.2018.e00530](https://doi.org/10.1016/j.heliyon.2018.e00530)



Integration of stationary wavelet transform on a dynamic partial reconfiguration for recognition of pre-ictal gamma oscillations

N. Jmail^{a,*}, M. Zaghoud^b, A. Hadriche^b, T. Frikha^c, C. Ben Amar^b, C. Bénar^d

^a *Miracl Laboratory, Sfax University, Sfax, Tunisia*

^b *REGIM Laboratory, Sfax University, Sfax, Tunisia*

^c *CES Laboratory, Sfax University, Sfax, Tunisia*

^d *Inserm, INS, Institut de Neurosciences des Systèmes, Aix Marseille University, Marseille, France*

* Corresponding author.

E-mail address: naweljmail@yahoo.fr (N. Jmail).

Abstract

To define the neural networks responsible of an epileptic seizure, it is useful to perform advanced signal processing techniques. In this context, electrophysiological signals present three types of waves: oscillations, spikes, and a mixture of both. Recent studies show that spikes and oscillations should be separated properly in order to define the accurate neural connectivity during the pre-ictal, seizure and inter-ictal states. Retrieving oscillatory activity is a sensitive task due to the frequency overlap between oscillations and transient activities. Advanced filtering techniques have been proposed to ensure a good separation between oscillations and spikes. It would be interesting to apply them in real time for instantaneous monitoring, seizure warning or neurofeedback systems. This requires improving execution time. This constraint can be overcome using embedded systems that combine hardware and software in an optimized architecture. We propose here to implement a stationary wavelet transform (SWT) as an adaptive filtering technique retaining only pre-ictal gamma oscillations, as validated in

previous work, on a partial dynamic configuration. Then, the same architecture is used with further modifications to integrate spatio temporal mapping for an early recognition of seizure build-up.

Data that contains transient, pre-ictal gamma oscillations and a seizure was simulated. The method on real intracerebral signals was also tested. The SWT was integrated on an embedded architecture. This architecture permits a spatio temporal mapping to detect the accurate time and localization of seizure build-up, while reducing computation time by a factor of around 40. Embedded systems are a promising venue for real-time applications in clinical systems for epilepsy.

Keywords: Biomedical engineering, Neurology

1. Introduction

One of the important techniques for the diagnosis of neurological diseases is the analysis of electrophysiological signal. These signals can be acquired either through electrical potentials (electroencephalography, EEG) or through magnetic fields (magnetoencephalography) in a non-invasive way. Epilepsy is one of the most frequent neurological diseases, and can be either controlled by medication or a surgical removal of epileptic regions. Thus, analyzing scalp electrophysiological signal (EEG, MEG) allows delineating the “epileptogenic zone” (EZ). The EZ is characterized by excessive excitability that may generate seizures; these discharges start from specific sources and propagate, involving large cortical areas forming networks [1, 2]. During pre surgical evaluation, the decision can be made to implant invasive electrodes in order to define the pathological tissues that need to be removed by surgery. Intracerebral EEG, electrocorticography (ECoG), and Foramen ovale EEG can thus be used to confirm the EZ localization before surgery. The success of surgery crucially depends on the signal-based biomarkers of the EZ. Two types of activities have been used: spikes (transient activities with high amplitude as defined by Gloor in 1975 [3]) and oscillations. For example, Oishi and his colleagues have relied on epileptic spikes localization [4], whereas Hiari and his colleagues proved the implication of different epileptic oscillations in the beta alpha theta and gamma bands [5]. Bragin proved that high frequency oscillations HFO could be also considered as markers of the EZ [6, 7, 8], which was confirmed by Urrestarazu and colleagues who confirmed that fast oscillations are the best hallmark of epileptogenic region. In order, to detect and characterize seizure onset, Ropun and his colleagues used a multi scale analysis of gamma-band oscillations [9]. Another separation method was proposed by Xiaoli based on empirical mode decomposition. This latter allowed showing that gamma oscillations are dominant during the pre-ictal state of an epileptic hippocampus in vivo [10]. Rojas confirmed that pre-ictal gamma oscillations are detectable from scalp EEG signal, and studying their network dynamics

may be useful in predicting seizure and novel seizure [11]. Meanwhile, Bénar and colleagues demonstrated that oscillatory and transient activities are difficult to separate as they overlap in the frequency domain. In particular, using simple filters may generate spurious oscillations that are simply the filter impulse response [12]. This potentially impacts the definition of epileptic networks, which can be a mixture of filtering spike and real oscillations.

In a previous work, several techniques were proposed to improve the separation such as Matching Pursuit (MP), Stationary Wavelet Transform (SWT) and adaptive models (“despiking”, i.e. removing transient activities). Their efficiency was evaluated on simulated data and real signals (IEEG, EEG foramen ovale and MEG), varying several parameters (signal to noise ratio, rate of overlap and occurrence, frequency range of oscillations, transient amplitude and width). However, these filtering techniques are expensive in computation time [13], and need to be improved for real time applications. In [10, 11], the importance of defining and studying pre-ictal gamma oscillations space and time presentation for early recognition and detection of seizure build up was emphasized. Nowadays, embedded systems have invaded large fields from industrial to health and healthcare area [14]. These embedded systems were dedicated to overcome time execution cost; hence much intelligent architecture were developed for preprocessing of physiological signal such as ECG MEG, EEG. The codesign techniques are very crucial in embedded system, providing the link between platforms (SoC, FPGA, ARM, ASIC) and coherent software. The design of embedded systems is a compromise between several constraints (cost, chip area, power consumption, and real-time) [15], thanks to a combination of hardware (processors, sensors, memories) and software (hidden intelligent routines). They allow achieving in real times many applications as highly secure neurologist decision support, autonomy and automatic intervention.

In this work the integration of SWT and spatio temporal mapping was proposed using a dynamic partial reconfiguration. Our goal was to implement real-time processing to predict seizure build-up, in order to construct in further work a new alerting device for detecting the early onset of seizures. The SWT was implemented [13] on an embedded system to separate in a convenient way pre-ictal gamma oscillations from transient spikes, with a minimum time of execution. In a second phase, the spatio temporal mapping of pure pre-ictal gamma oscillations for early seizure recognition was integrated.

2. Materials and methods

2.1. Materials

The simulated data and all signal processing were done using the Matlab software (Mathworks, Natick, MA) and the EEGlab toolbox [16]. The implementation of

mixed architecture was embedded on a Xilinx Virtex 5 ML 505 platform, using Matlab and HDL toolbox, as presented in Fig. 1.

2.1.1. Simulations

Our simulated data was inspired from real intracerebral EEG signal of a pharmaco resistant epileptic patient. Three channels were simulated with a 256 Hz sampling frequency, depicting three types of occurrence between transient and pre-ictal gamma oscillations: activities separated, partially overlapping and fully overlapping. Pre-ictal gamma oscillations frequency was set to 45, 55 and 85 Hz for channel 1, 2 and 3 respectively, and a colored noise, was added as in [17]. The time occurrence of transient activity was each 0.8 s with a jitter <40 ms: 200 realizations were generated varying the noise.

2.1.2. Real signal

A pre surgical intracerebral EEG signal from a pharmaco resistant subject with a symptomatic focal cortical dysplasia in the right occipito-temporal junction was investigated. The implantation technique was Stereotaxic EEG (SEEG), consisting

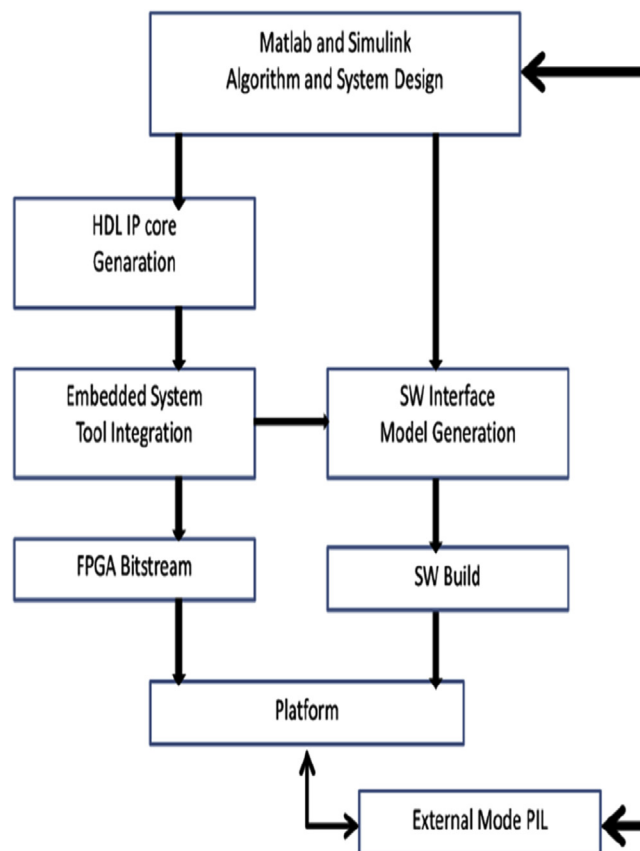


Fig. 1. Materials for implementation procedure.

in depth electrodes. The acquisition and preprocessing phases were applied in the Clinical Neurophysiology Department of 'La Timone hospital' in Marseille as in [13] studied and validated by an expert neurologist. This particular IEEG recording was chosen because it presented clear pre-ictal patterns with regular spiking and visible epileptic oscillations as validated by the expert. Accurate position of depth electrodes was defined upon a non-invasive phase that allows defining a putative epileptogenic zone (ZE). The IEEG data was recorded on a Deltamed System, sampled at 256 Hz, with anti-aliasing low-pass analog filter set to 100 Hz. Eight multi-contact depth electrodes of 0.8 mm diameter, 10–15 contacts, each 2 mm long with an inter-contact distance of 1.5 mm, were positioned in the right hemisphere, implanted according to Talairach's stereotaxic method (Talairach and Bancaud 1973). Our data set is composed of 3 min 20 second with 96 channels and 4 events.

Patients signed informed consent, and the Institutional Review board (IRB00003888) of INSERM (IORG0003254, FWA00005831 has approved the study.

2.2. Methods: SWT as a case study

The stationary wavelet transform SWT is a filtering technique that relies on time and scale signals representation. The stationary property ensures time invariance: a translated version of a signal X leads to a translation of its transformation. This is thus an effective tool for spontaneous signals representation, separation, detection and filtering processes [18]. In fact, The redundancy of SWT leads to translation-invariance, which is an interesting property as spontaneous oscillations are not always aligned to the same 'tiles' of the time-frequency plane. This, it facilitates salient signal features identification, as in continuous wavelet transform, as oscillations are more easily separated from the high frequency part of the transient spikes. Interestingly, and contrary to the continuous wavelet transform, the SWT is a reversible technique, as the discrete wavelet transform DWT, which allow to reconstruct the inverse function ISWT (from selected coefficient to a filtered dataset).

SWT was chosen among several decomposition techniques because of its demonstrated advantages for overcoming the frequency overlap between gamma rhythms and transient activities [13]. Other techniques such empirical mode decomposition ([19]), and even variational mode decomposition are based essentially on defining the central frequency of each events which wouldn't be effective in separating activities sharing the same central frequency, this hypothesis is in contradiction with our study [20]. Although, Tunable -Q wavelet transform has been proved as a powerful tool for EEG oscillatory signal analysis, since it controls the oscillation of the used wavelet for a sub band frequency, but it remains effective only for separated sub band activities. Hence, Tunable -Q wavelet transform would not separate our studied activities since these activities have common component in the same sub band frequency [21].

The SWT was derived from the discrete wavelet transform DWT (obtained through a step of convolution followed by a decimation) but without down sampling the scales [22]. The SWT of a signal X is the convolution product of X and filters (a lowpass then a highpass) that procures the approximation $C_{j,k}$ and detail coefficients $W_{j,k}$ consecutively at the j level. These coefficients are obtained by adapting two scale functions φ_k and Ψ_k fitted in time (by translation, compression and dilatation) as expressed in the following Eqs. (1) and (2):

$$\begin{aligned} C_{j,k} &= \langle X(t)\varphi_k(t) \rangle \\ W_{j,k} &= \langle X(t)\Psi_k(t) \rangle \end{aligned} \quad (1)$$

$$\begin{aligned} \varphi_k(t) &= 2^{-j}\varphi(2^{-j}(t-k)) \\ \Psi_k(t) &= 2^{-j}\Psi(2^{-j}(t-k)) \end{aligned} \quad (2)$$

After a decomposition step, the transient components were selected from oscillatory ones. In this study, the separation between pre-ictal gamma oscillations and transient activities in order to perform an early recognition of seizure build up was investigated. More precisely, non contaminated pre-ictal gamma oscillations spatio temporal representation were carried out as in [17]. A thresholding step based on a rectangular mask with a time spread equal to gamma oscillatory length (200 ms for 45 Hz, 180 for 55 Hz and 150 ms for 85 Hz) and 3 to 2 scales of width (3 scales for 45 Hz and 2 scales for the rest) was used as in [13]. The last step of separation is the reconstruction of thresholded coefficients (masked approximation and detail coefficients) using the inverse function ISWT on matlab.

The SWT performance for separating transient and oscillatory activities was studied in previous work [13]. For simulated data the SWT goodness of fit (match between separated recovered activities and simulated ones) was shown to be above 80%, and it depends of the frequency range of oscillations (in our case the separation is above 90%: gamma rhythms), and signal to noise ratio. For electrophysiological signal SWT provided the best results in terms of consistency across peaks of oscillatory source localization compared with FIR and MP filtering techniques, also for automatic gamma oscillations detection, SWT F score measure is between 0.83 for 45 Hz and 0.93 for 85 Hz on 4 hours of simultaneous Foramen Ovale and scalp EEG recordings, hence SWT have been evaluated as a robust and a promoting technique in separation between transient and oscillatory activities with minor false alarm in order to predict a seizure build up.

3. Theory/calculation

SWT can be implemented based on a convolution step, which is heavy in computation. the use of two filters in parallel (a high pass and low pass), would ensure 50% gain in time cost execution [22]. The results of filtering step are thresholded to detect

only pure oscillatory components. Firstly, the adapted architecture was studied for SWT integration, then the chosen platform was described and finally our proposed embedding architecture of gamma reconstruction and spatio temporal mapping in order to predict seizure build-up was demonstrated.

3.1. Embedded architecture

An adaptive architecture based on a partial dynamic reconfiguration was applied [23]. This reconfiguration approach has been shown to overcome the complexity of spatial mapping routines [15] with a minimum hardware even for multiple implementations [24].

Integrating a filtering technique requires both local and large scale infrastructures with many constraints that affect the actual separating results. The adopted architecture used in our case (a static and dynamic bloc) is characterized by a high level of flexibility (further modifications could be applied even after execution), and less temporal dissipation during the execution process [25]. In this work, two accelerators on VHDL were used, (to control static and dynamic blocs), linked via a Macros Bus. Memory rings were associated to these processors to save the separation results (Filtering, thresholding results), sent back to processor via FSL, and finally, saved in an external memory unit [26]. The separated activities will be displayed in the future on a terminal screen connected to the used FPGA. A control unit for start was used (to generate accurate address among memory units) and for finish (to store output signals of separation algorithm). A Microblaze processor (32-bit embedded micro-processor) was integrated to overview the separation data path units and the results transfers. On the other hand, for dynamic bloc, two bits streaming were used as in [27], with a power PC hardcore processor, which can reach 150 MHz (a reconfigurable module that operates at the static module frequency = 150 MHz), then a mono-core was added to handle the multiple iteration of our separation routine [23].

3.2. Chosen platform

The hardware/software codesign approach of our application was applied on Xilinx Virtex-5ML505 (an Embedded Development Kit EDK software and FPGA XC5VLX50T-1FFG1136). The Xilinx Virtex-5ML505 features a large numbers of Input/Output peripherals and an important memory storage that allows a high level of smart development of connected, and differentiated systems.

3.3. Demonstration

For simulated data the SWT is iterated $3*200 = 600$ times and for real signal $96*4 = 384$ (number of channel by realizations/events) times. Our algorithm could be explained through two rings: a data vector, and a correlation process, proceeding in

a parallel way. A data vector contains a window of 5000 samples: 20 s, for both simulated and real IEEG signal with an amplitude range of $[-20\ 30]\ \mu\text{v}$, which lead to 50 values stored in a multi IO memory [28]. Our original signal was convolved with two filters φ_k and Ψ_k , followed by a thresholding step using a rectangular shape transfer function (see Eq. (3)). The final results were added and stored in a memory bloc using MATLAB Simulink with Xilinx system generator library for VHDL files generation and required netlist.

$$\begin{aligned} thre_d &= \langle C_d, \text{rect} \rangle, \\ thre_a &= \langle C_{ad}, \text{rect} \rangle \end{aligned} \quad (3)$$

With $thre_d$ and $thre_a$ are the SWT details and approximate coefficients in our rectangular mask adopted for oscillatory activities.

3.4. Spatio temporal representation

The Morlet wavelet transform was used to depict a spatio temporal map of pure pre-ictal gamma oscillations. The Morlet wavelet is the classical one used in neuroscience [12]. These wavelets provide a good compromise between time and frequency resolution. Other wavelets could be used (see [29]).

In fact, convolving IEEG signals with Morlet wavelets (Gabor atoms with oscillation parameter $\xi = 5$ parameters) gives condensed activities in the time-frequency domain and a good adjustment between time and frequency resolution.

Morlet wavelets are obtained from translating and dilating (time and scale shifting) the mother wavelet function [30] (a complex exponential modulated by a Gaussian envelop) defined in Eq. (4):

$$\Psi(t) = \exp(iw_0 t) \exp\left(-\frac{t^2}{2s^2}\right) \quad (4)$$

W_0 denotes the frequency and s is a measure of spread, Ψ is shifted in time and scale by (a, b) values as expressed in Eq. (5)

$$\Psi_{(b,a)}(t) = 1/a \exp\left(iw_0 \left(\frac{t-b}{a}\right)\right) \exp\left(-\frac{\left(\frac{t-b}{a}\right)^2}{2s^2}\right) \quad (5)$$

As in [13], a convolution between pure pre-ictal gamma oscillations and a moving average function with 256 width was applied [31] to smooth the pure gamma oscillations envelope fluctuation [32]. Finally a normalization step was implemented by the lower frequency band as in [2].

3.5. Integrating spatiotemporal analysis

The integration of spatio temporal map on an embedded architecture, was proceed as for the SWT integration; using a dynamic partial reconfiguration (Section 3.3), manipulated by the FPGA Xilinx Virtex-5ML505. The data vector bloc was kept and further modifications were made for the correlation bloc. Three blocks were implemented: one to compute the Morlet transform in cascade with a second unit which treats the smoothing operation and the last ring is dedicated for normalization. The results will be saved in a memory bloc, and then delivered to a terminal screen where time and space seizure build up was recognized.

These processes are described by the following equations:

$$\begin{aligned} C_{(a,b)}(nT_e) &= X(nT_e) * \Psi_{(b,a)}(nT_e) \\ S_{(a,b)}(nT_e) &= C_{(a,b)}(nT_e) * \sin(2\pi nT_e) \\ Z_{(a,b)}(nT_e) &= S_{(a,b)}(nT_e) * H(nT_e) \end{aligned} \quad (6)$$

With C is Morlet transform, S denotes smoothing the C transform via a sinusoidal envelope, H is the transfer function of a band pass filter and Z is the normalized signal.

4. Results and discussion

Our simulated data is inspired from a focal epileptic IEEG signal, which presents a pre-ictal and a seizure state. Three channels are generated with a mixture of transient and pre-ictal gamma activities at 45, 55 and 85 Hz. Signals are depicted in Fig. 2, along with real IEEG signal for a 20 s window.

In Fig. 3, the processing steps to separate transient spikes and pre-ictal gamma oscillations were illustrated using SWT filter technique. Then the pure pre-ictal gamma oscillations were shown in a spatio temporal mapping.

Firstly, SWT was applied for each channel, then thresholding step was used and finally, pure pre-ictal gamma oscillations were recovered. Processing was applied both to simulations and real IEEG signals. For spatio temporal mapping, the energy of all the involved channels (for both simulated data and real IEEG signal) were computed before and after retrieving all transient activities to define build up of pure pre-ictal gamma oscillations.

The reconstruction of pre-ictal gamma oscillations among original signal, using two different masks shapes was depicted in Fig. 4. A rectangular mask was adopted (length and width are function of frequency range) for oscillations and a pyramidal mask for transients.

In Fig. 5 pre-ictal 55 Hz gamma oscillations reconstruction was demonstrated. The original IEEG signal and the recovered gamma oscillations during pre-ictal and seizure states were illustrated.

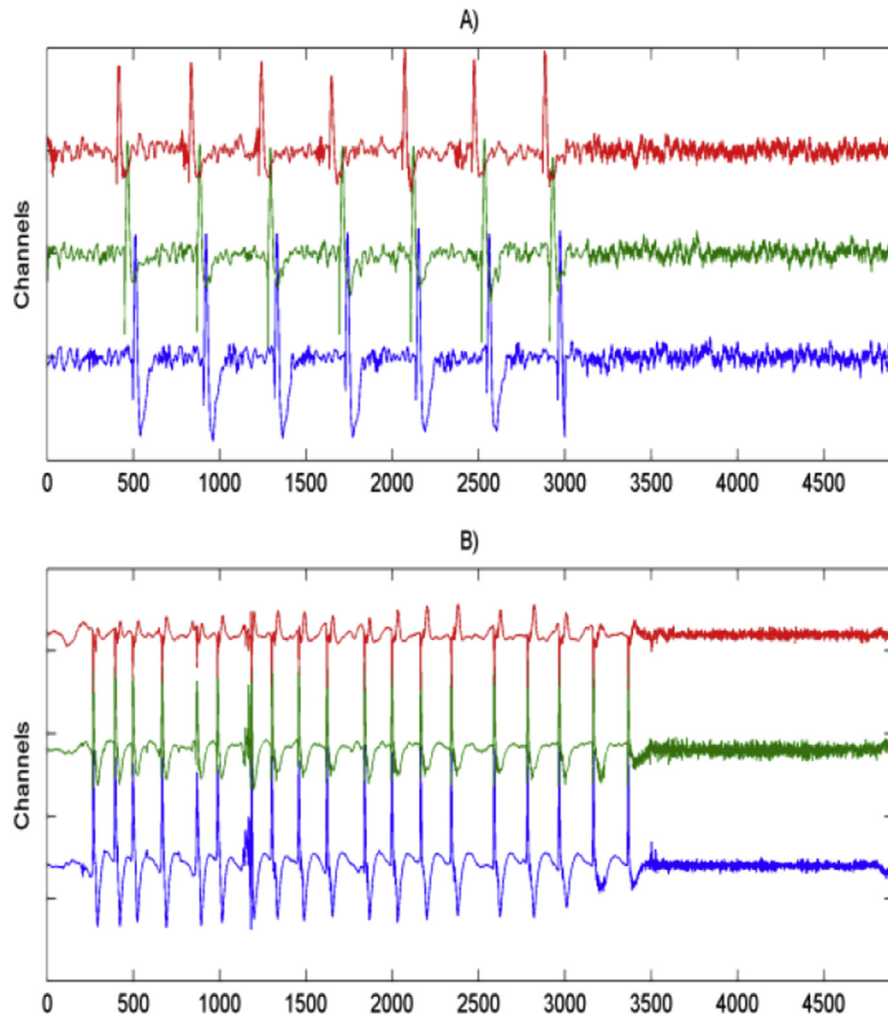


Fig. 2. A) One realization of simulated data, with 3 cases of overlap between transient and oscillations of 45, 55, and 85 Hz frequency, preceded by a seizure state. B) Three channels of IEEG signal with transient, pre-ictal gamma oscillations of 45–85 Hz and seizure state.

The spatio temporal maps were depicted in Fig. 6, for 85Hz pre-ictal gamma oscillations, across all channels of our IEEG signal. A time window of 20 s (15s pre-ictal state 5 s of seizure) normalized (by dividing with energy of band-passed signal at 80–90 Hz) and smoothed was used. The seizure build-up is clearer for signal with only pre-ictal gamma oscillations (no transient activities overlapping with gamma oscillations) which indicates that large energy of spikes hampers the characterization of pre-ictal states. Several channels present high energy in the chosen frequency band during seizure build up. Hence, pre-ictal oscillations may be considered as a complementary biomarker of the epileptogenic zone.

Fig. 7 depicts the integration of dynamic partial reconfiguration for our adopted separation technique (SWT plus thresholding). Partial reconfiguration contains two

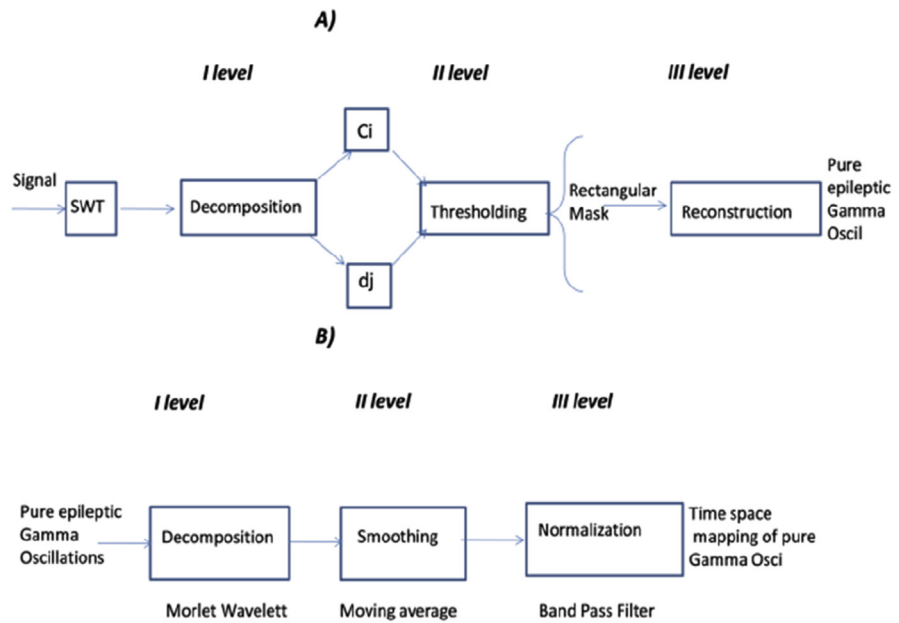


Fig. 3. Steps for separating between transient spikes and gamma oscillations by SWT and producing spatio-temporal mapping of pure gamma oscillations.

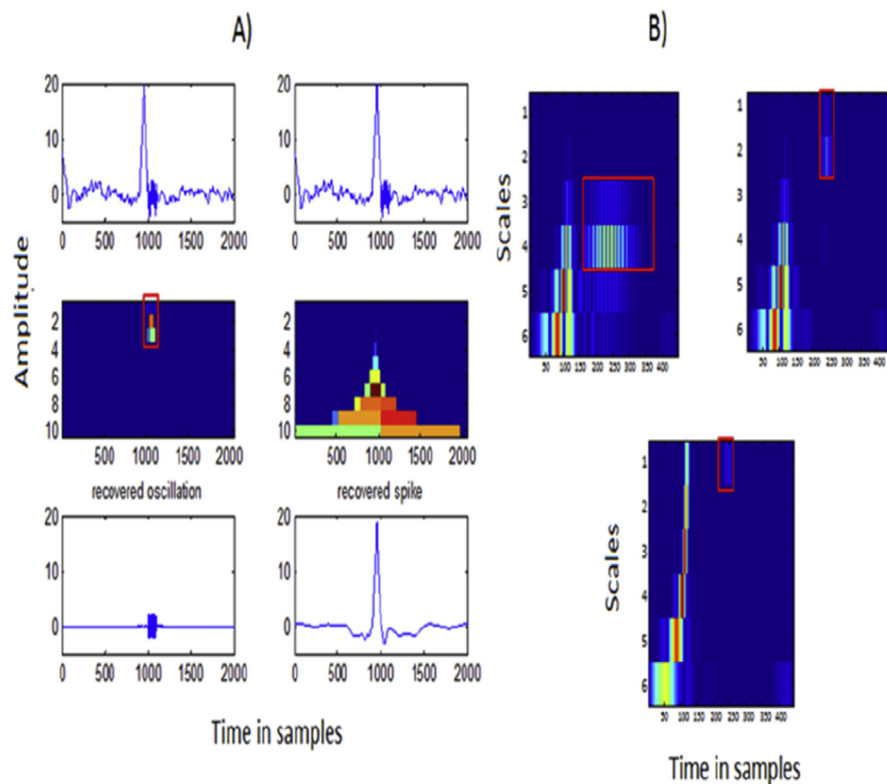


Fig. 4. A) line 1: Mixture of a simulated spike and a gamma oscillation of 45 Hz with full temporal overlap, line 2: masks used for thresholding transient among oscillations, line 3 recovered gamma oscillations and transient spikes by SWT. B) SWT approximation coefficients for 45, 55, 85 Hz oscillations: a rectangular mask to recover only oscillatory components.

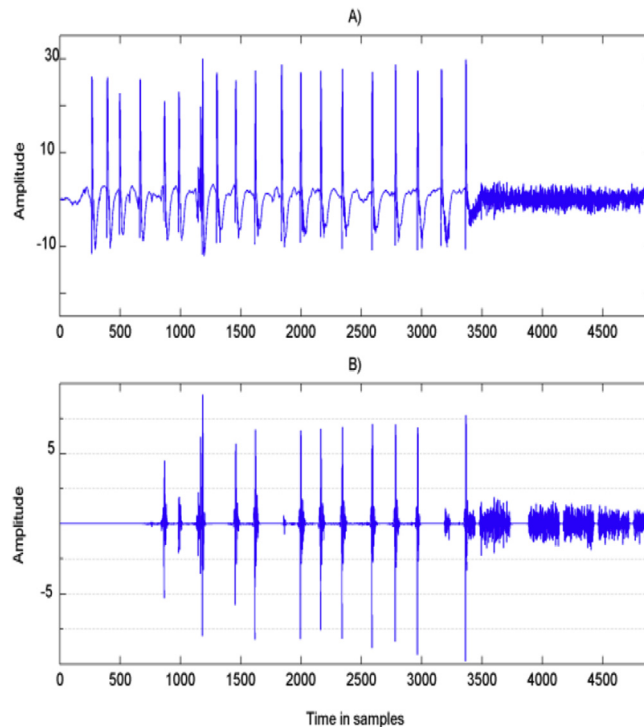


Fig. 5. A) IEEG signal: a mixture of transient and pre-ictal gamma activities. B) Reconstructed pre-ictal gamma oscillations by SWT.

blocks, a static and a dynamic one, connected to a Microblaze and an external memory unit via a Macros Bus.

Fig. 8 presents our adopted architecture for integrating the separating technique. It is composed of a data vector block and a correlation block. The correlation unit is the most important part of the adopted architecture. It is independent of the other blocks; translating three convolution operations to keep only oscillatory components from an original signal. Thus, 3 sets of addition and multiplication operators were used. Each set is dedicated to a convolution operation (down-sampling scale functions, decomposition and thresholding). Multiplication and addition operations are set in a parallel way: the first operation deals with down-sampling scale function, second operation is dedicated for convolution between pre-ictal signal (simulated and real IEEG) and two adopted filters transfer functions (scale function) which results in two types of coefficients (approximation and detail coefficients). The last operation, the thresholding process, performs multiplication of the SWT coefficients by rectangular Masks. These convolution operation Blocks will be executed in parallel since we integrated 2 accelerators as in [28]. The preprocessing results will be stored in two separated internal memory (Msd/Msa for scaling function, Md/Ma: approximation and detail coefficient and Mat/Mdt for thresholded approximation and detail coefficients). Then, the oscillatory components will be added and saved in an external

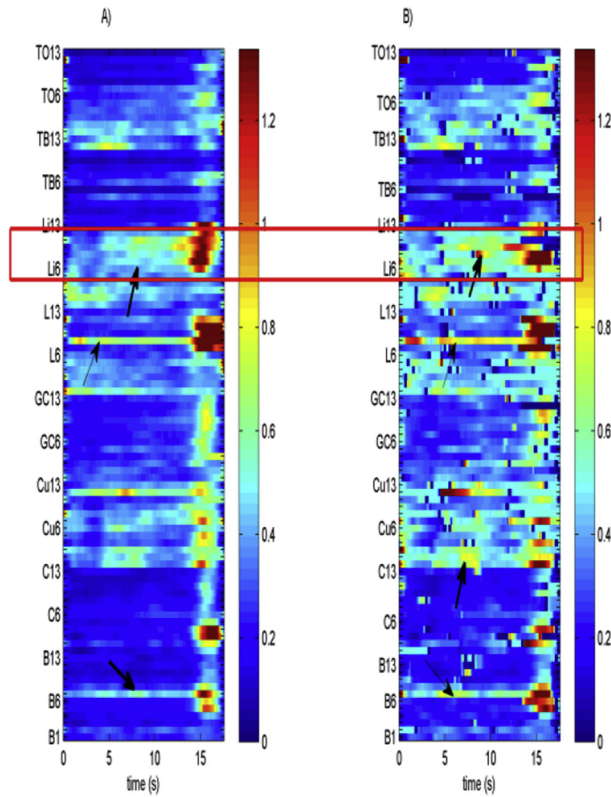


Fig. 6. A) IEEG spatio temporal mapping: no clear pattern in the pre-ictal period (before $t = 13s$). B) IEEG spatio temporal map of pure gamma oscillations: a clear ‘build-up’ of oscillatory activity can be seen in channels Li, L and B (black arrows and red rectangle).

Memory block, which will store only pure pre-ictal gamma oscillatory components for simulated data or real IEEG signal, incoming firstly from the data vector bloc, in order to be ruled by the correlation unit described above.

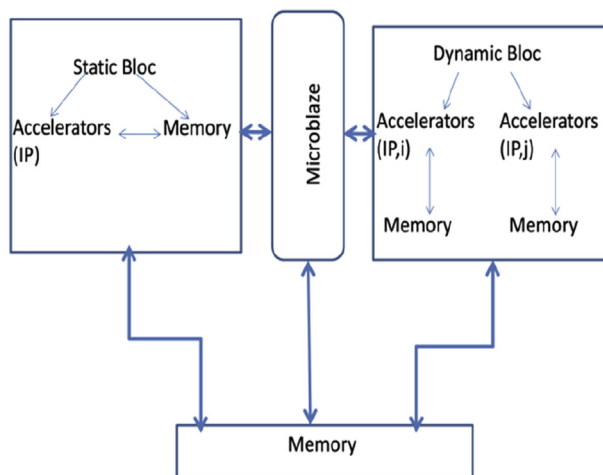


Fig. 7. Partial reconfiguration: a static and dynamic bloc connected to a Microblaze and external memory. The static block is handled by accelerators and memory for instantaneous saving; the dynamic unit contains two accelerators and memories.

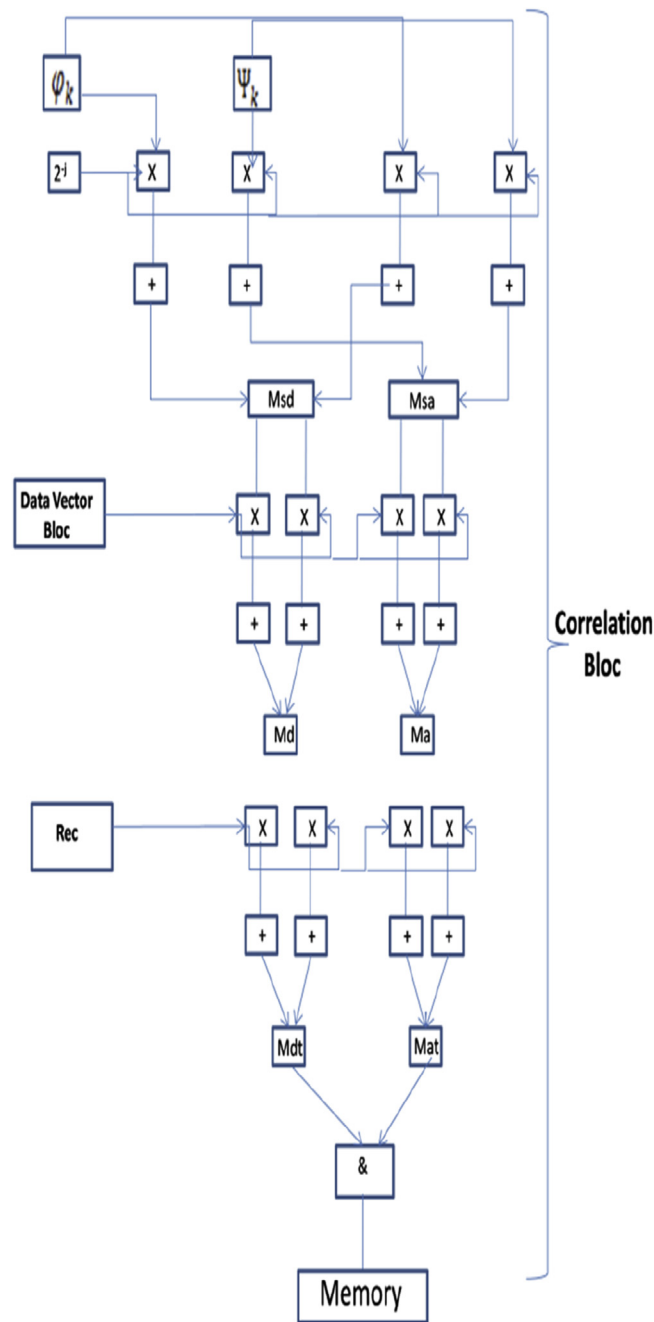


Fig. 8. Integration of adopted architecture of separating technique: a data vector to receive and save input signal and correlation bloc which contains 3 operations sets: multiplication/addition, 3 internal memories and an external memory to restore only pure pre-ictal oscillations.

Our algorithm was profiled to recover pure pre-ictal gamma oscillations without accelerators, then with the integration of 2 accelerators (as described in the section above). A stimulation test in Xilinx ISE was run; [Table 1](#) depicts our algorithm time consumption. Adding 2 accelerators has alleviated execution consumption by

Table 1. Time consumption of integrating SWT.

SWT Integration	Time per Tics
Software	420
No Accelerator	45
2 Accelerators	23

about 400 times per tics comparing with SWT software, and 22 tics of time gain was obtained in comparison to a solution without accelerator.

Fig. 9 illustrates the integration of pre-ictal gamma oscillations spatio temporal mapping. Our adopted platform is composed of three blocks, each one involving three sets of convolution (Morlet transform, smoothing and normalization). Each block

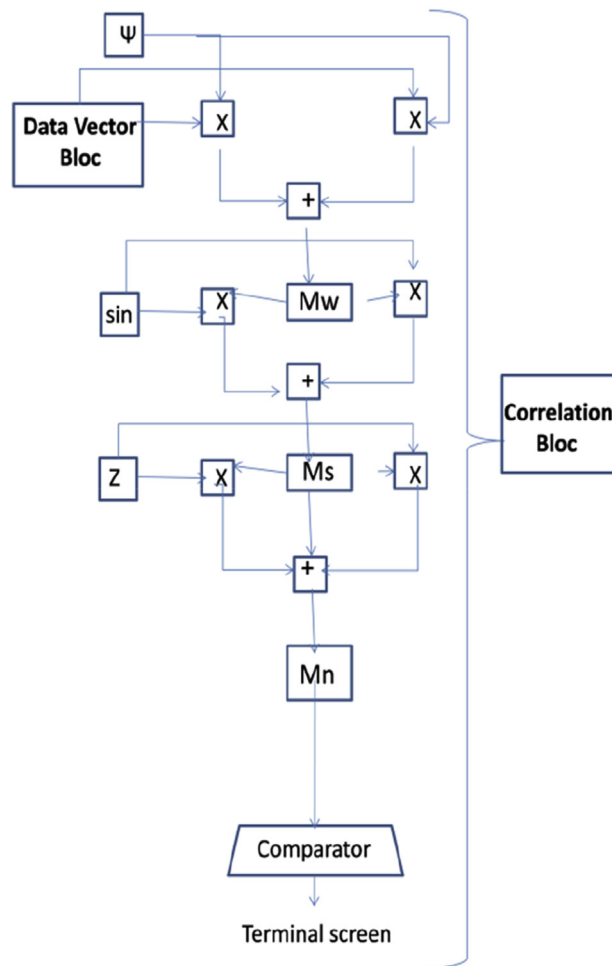


Fig. 9. Integration of spatio temporal mapping: a data vector, a correlation block with three convolution sets. The resulting data will be incorporated into a comparator to display the highest energy in space and time (in order to detect the seizure build up in real time).

Table 2. Time consumption of spatio temporal mapping STM.

Embedding STM	Time per Tics
Software	320
No Accelerator	35
2 Accelerators	16

is composed of addition and multiplication operators, linked to an internal memory unit to store the results (Mw for wavelet transform, Ms for smoothing and Mn for normalization). The input Ψ , H, sin and Z denote the used transfer functions. After compiling, a comparator was used to detect the sensors' maximum energy. Final output result would be stored in an external memory unit then mapped on a screen.

Embedding spatio temporal mapping was profiled using the same architecture for SWT integration: a dynamic partial reconfiguration on Xilinx platform, composed of a data vector bloc to access the input signal (original signal/pure gamma) and a correlation block with three multiplication/addition rings, 3 memory units and an external memory bloc to store the highest energetic component of the involved sensors during seizure build-up.

Table 2, collects time consumption for embedding pre-ictal gamma oscillations spatio temporal mapping (STM). As demonstrated in the first table, it is clear that using 2 accelerators made about also 20 tics of time gain compared without accelerators and about 304 times per Tic in comparison with classical software.

Table 3, represents the time consumption in slices/flip flop slices and BRAM for the entire integration procedure (from separating pre ictal gamma oscillations to spatio temporal mapping) using Xilinx ML 505 Platform Studio. This allowed us to define the proposed embedding system exploitation rate for our proposed system.

Logic uses rate is about 70% of the available capacity, which demonstrates a good exploitation of our proposed embedded architecture for the integration of an early recognition system of seizure build up.

Finally, **Table 4** presents the embedding system power consumption used for integrating our application. The required energy for this procedure is acceptable for

Table 3. Integration of recognition seizure build up: Logic uses.

Logic study	Available	Hold	Rate %
Slices	7616	11200	68
Flip Flops Slices	28224	44800	63
BRAMS	144.5	228	63.5

Table 4. Power consumption for integrating the recognition of seizure build-up.

Integrating procedure	Power consumption
No accelerator	1480 mW
Two accelerators	3000 mW

embedding systems and Xilinx platform, even after adding two accelerators. A simple battery is sufficient to supply power to our used algorithm.

Although the power consumption of integrating our algorithm with two accelerators is about twice the power required without accelerator, the consumption is still low and acceptable among the integration field. Hence, using two accelerators seems to be the best compromise for integrating our algorithm since they have an important impact on time gain consumption and did not set too much pressure on power supply.

5. Conclusion

Early recognition of epileptic seizure is an important task in epilepsy diagnosis, especially for pharmaco-resistant patients. The analysis of electrophysiological (EEG, MEG, EEGFo, IIEEG, ECoG) is fundamental in this field. Importantly, these signals show a mixture of activities (transient waves and oscillations) which potentially imply different cortical regions. In a previous work, the difficulty of separation between these activities was emphasized and reliable filtering techniques was suggested, evaluated against several constraints [1, 12, 13, 17, 33]. Among these techniques, SWT was shown to be a convenient tool for the separation between transient and oscillations. The capacities of SWT filtering technique in separating gamma oscillation and transient activities has been tested using the ROC method. We have shown that the F score measure (combining true and false alarms) ranged between 0.83 for 45 Hz and 0.93 for 85 Hz on 4 hours of simultaneous Foramen Ovale and scalp EEG recordings. In this study, SWT was applied to remove transient activities and keep only pure pre-ictal gamma oscillations in simulated and IIEEG signal. The recovering of non contaminated pre-ictal gamma oscillation was firstly validated on simulated data inspired from epileptic IIEEG signal, then on focal epileptic IIEEG data. Pure gamma activities spatio temporal mapping lead to a better characterization of accurate time and localization of excessive discharges. Hence, the responsible regions and the dynamic time of seizure build-up would be predicted (in agreement with previous work, [17]). However these pre processing steps are heavy in computation, which called for integrated systems, to perform real time processing. SWT was embedded on a dynamic partial reconfiguration based on a static and a dynamic block, which improved drastically time execution. The same results of separation were maintained with almost 400 times acceleration than classical implementation. Our proposed embedded system is based on a data vector block and a correlation unit. The correlation block is made of 3 memory units (to

store results of convolution) and 3 sets of addition and multiplication operators to profile the convolution operation. In a second step, a spatio-temporal mapping of non-contaminated pre-ictal gamma oscillations was implemented using the same adopted architecture and reconfiguration as those exploited for the SWT integration. An external memory unit was linked to the FPGA to save the pre-ictal gamma oscillations energy and, finally, mapped on a screen. Two accelerators were managed for each integration process to reduce time consumption and to increase the logic manipulation in our adopted architecture. Our proposed architecture reaches almost 70% of the available capacity and 700 ticks gain in total computation costs. The power consumption is also convenient for Xilinx platform, even when two accelerators were added; a simple battery can handle the power supply of our proposed system. These results could help neurologists in an early seizure recognition and detection, and could be also implemented in a portable device for epileptic subjects to alarm them about seizure build up, in order to take necessary precautions to reduce risks before seizure state. Another application would be in a real time neurofeedback system.

Although promising, our proposed study still has some limitations and need further improvement. Further work will evaluate SWT automatic pre-ictal gamma oscillation detection on multiple data sets for checking robustness. A comparison between the robustness of recovering pre-ictal gamma oscillations by SWT against despiking as developed in [17] is suggested to evaluate the performances in terms of time consumption and power supply. The dynamics network activations of pre-ictal gamma oscillations in order to define precisely the best markers of seizure build-up should be also investigated. All the resulting routines should be in second step integrated to propose both neurofeedback and monitoring devices. These devices are expected to help reducing immediate danger arising from seizure, and improving patient care.

Declarations

Author contribution statement

Nawel Jmail: Conceived and designed the experiments; Performed the experiments; Analyzed and interpreted the data; Wrote the paper.

Abir Hadriche, Chokri Ben Amar: Conceived and designed the experiments.

Ridha Jarray, Tarek Frikha: Performed the experiments.

Christian Benar: Analyzed and interpreted the data; Contributed reagents, materials, analysis tools or data.

Funding statement

Nawel Jmail was supported by the SSHN grant from the Institut Français de Tunisie.

Competing interest statement

The authors declare no conflict of interest.

Additional information

No additional information is available for this paper.

Acknowledgements

The authors thank Martine Gavaret for useful discussions. The authors also wish to thank the anonymous reviewers for their useful comments.

References

- [1] N. Jmail, M. Gavaret, F. Bartolomei, P. Chauvel, J.M. Badier, C.G. Bénar, Comparison of brain networks during interictal oscillations and spikes on magnetoencephalography and intracerebral EEG, *Brain Topogr.* 29 (5) (2016) 752–765.
- [2] F. Bartolomei, P. Chauvel, F. Wendling, Epileptogenicity of brain structures in human temporal lobe epilepsy: a quantified study from intracerebral EEG, *Brain* 131 (7) (2008) 1818–1830.
- [3] V. Diekmann, et al., Localisation of epileptic foci with electric, magnetic and combined electromagnetic models, *Electroencephalogr. Clin. Neurophysiol.* 106 (1998) 297–313.
- [4] M. Oishi, H. Otsubo, S. Kameyama, N. Morota, Epileptic spikes: magnetoencephalography versus simultaneous electrocorticography, *Wiley Online Libr.* 43 (11) (2002) 1390–1395.
- [5] N. Hirai, S. Uchida, T. Maehara, Y. Okubo, H. Shimizu, Enhanced gamma (30–150 Hz) frequency in the human medial temporal lobe, *Neuroscience* 90 (4) (1999) 1149–1155.
- [6] A. Bragin, C.L. Wilson, R.J. Staba, M. Reddick, I. Fried, J. Engel, Interictal high-frequency oscillations (80–500Hz) in the human epileptic brain: entorhinal cortex, *Ann. Neurol.* 52 (4) (2002) 407–415.
- [7] E. Urrestarazu, R. Chander, F. Dubeau, J. Gotman, Interictal high-frequency oscillations (10–500 Hz) in the intracerebral EEG of epileptic patients, *Brain* 130 (9) (2007) 2354–2366.
- [8] A. Bragin, J. Engel Jr., C.L. Wilson, I. Fried, G. Buzsaki, High-frequency oscillations in human brain, *Hippocampus* 9 (2) (1999) 137–142.

- [9] K. Roopun, et al., Detecting seizure origin using basic, multiscale population dynamic measures: preliminary findings, *Epilepsy Behav.* 14 (Suppl 1) (2009) 39–46.
- [10] X. Li, J.G.R. Jefferys, J. Fox, X. Yao, Neuronal population oscillations of rat hippocampus during epileptic seizures, *Neural Network.* 21 (8) (2008) 1105–1111.
- [11] C. Alvarado-Rojas, et al., Slow modulations of high-frequency activity (40–140Hz) discriminate preictal changes in human focal epilepsy, *Sci. Rep.* 4 (2014) 4545.
- [12] C.G. Bénar, L. Chauvière, F. Bartolomei, F. Wendling, Pitfalls of high-pass filtering for detecting epileptic oscillations: a technical note on ‘false’ ripples, *Clin. Neurophysiol.* 121 (3) (2010) 301–310.
- [13] N. Jmail, et al., A comparison of methods for separation of transient and oscillatory signals in EEG, *J. Neurosci. Methods* 199 (2) (2011) 273–289.
- [14] R. Devarajan, S.C. Jha, U. Phuyal, V.K. Bhargava, Energy-aware user selection and power allocation for cooperative communication system with guaranteed quality-of-service, in: *12th Canadian Workshop on Information Theory, CWIT 2011*, 2011, pp. 216–220.
- [15] J.-P. Diguët, Y. Eustache, G. Guy, Closed-loop–based self-adaptive hardware/software-embedded systems: design methodology and smart cam case study, *ACM Trans. Embed. Comput. Syst.* 10 (3) (2011) 221–252.
- [16] A. Delorme, S. Makeig, EEGLAB: an open source toolbox for analysis of single-trial EEG dynamics including independent component analysis, *J. Neurosci. Methods* 134 (1) (2004) 9–21.
- [17] N. Jmail, M. Gavaret, F. Bartolomei, C.-G. Bénar, Despiking SEEG signals reveals dynamics of gamma band preictal activity, *Physiol. Meas.* 38 (2) (2017) N42–N56.
- [18] X.H. Wang, R.S.H. Istepanian, Microarray image enhancement by denoising using stationary wavelet transform, *IEEE Trans. NanoBiosci.* 2 (4) (2003) 184–189.
- [19] S. Hiremani, D.A. Torse, N.J. Inamdar, Classification of EEG signals using Empirical Mode decomposition and Neural networks, 2015, pp. 224–231.
- [20] K. Dragomiretskiy, D. Zosso, Variational mode decomposition, *IEEE Trans. Signal process* 62 (3) (2014) 531–544.

- [21] R. Hassan, M.I.H. Bhuiyan, A decision support system for automatic sleep staging from EEG signals using tunable Q-factor wavelet transform and spectral features, *J. Neurosci. Methods* 271 (2016) 107–118.
- [22] E. Matsuyama, D. Sai, Y. Lee, N. Takahashi, Comparison of a discrete wavelet transform method and a modified undecimated discrete wavelet transform method for denoising of mammograms, in: *Conf Proc IEEE Eng Med Biol Soc*, 2013, pp. 3403–3406.
- [23] G. Simon, P. Volgyesi, M. Maroti, A. Ledeczki, Simulation-based optimization of communication protocols for large-scale wireless sensors networks, in: *Proceedings of the IEEE Aerospace Conference*, 2003, 2003, pp. 1339–1346.
- [24] S. Raaijmakers, S. Wong, Run-time partial reconfiguration for removal, placement and routing on the Virtex-II Pro, in: *Proceedings - 2007 International Conference on Field Programmable Logic and Applications, FPL*, 2007, pp. 679–683.
- [25] L.K. Demingny, B. Bourguiba, How to use high speed reconfigurable fpga for real time image processing, in: *IEEEConf. On Computer Architecture for Machine Perception*, IEEE Circuit and Systems, 2006, 2006, pp. 240–246.
- [26] A. Ghorbel, N. Ben Amor, M. Jallouli, Towards a parallelization and performance optimization of Viola and Jones algorithm in heterogeneous CPU-GPU mobile system, in: *International Conference on Intelligent Systems Design and Applications*, IEEE ISDA 2015, 2015, pp. 529–533.
- [27] T. Frikha, A. Hadriche, R. Khemakhem, N. Jmail, M. Abid, Adaptive architecture for medical application case study: evoked Potential detection using matching pursuit consensus, in: *International Conference on Intelligent Systems Design and Applications*, IEEE ISDA, 2015, pp. 576–580.
- [28] T. Frikha, N.B. Amor, K. Lahbib, J.P. Diguët, M. Abid, A data adaptation approach for a HW/SW mixed architecture (case study: 3D application), *WSEAS Trans. Circuits Syst.* 12 (9) (2013) 263–272.
- [29] R. Zelman, M. Zijlmans, J. Jacobs, C. Chatillon, J. Gotman, Improving the identification of high frequency oscillations, *Clin. Neurophysiol.* 120 (2009) 1457–1464.
- [30] S.P. Addison, *The illustrated wavelet transform handbook: introductory theory and applications in science engineering, medicine and finance*, Bristol Inst. Phys. Publ. (2002) 353.
- [31] O. David, et al., Imaging the seizure onset zone with stereo-electroencephalography, *Brain* 134 (10) (2011) 2898–2911.

- [32] M. Le Van Quyen, et al., Comparison of Hilbert transform and wavelet methods for the analysis of neuronal synchrony, *J. Neurosci. Methods* 111 (2) (2001) 83–98.
- [33] N. Jmail, M. Gavaret, F. Bartolomei, C.G. Benar, Despikifying SEEG signals using a temporal basis set, in: *International Conference on Intelligent Systems Design and Applications, ISDA IEEE, 2015, 2016*, pp. 580–584.